Earthq Eng & Eng Vib (2011) 10: 51-64 **DOI**: 10.1007/s11803-011-0046-4

A family of explicit algorithms for general pseudodynamic testing

Shuenn-Yih Chang†, Yuan-Sen Yang‡ and Chi-Wei Hsu§

Department of Civil Engineering, Taipei University of Technology (NTUT), NTUT Box 2653, Taipei 106, Chinese Taipei

Abstract: A new family of explicit pseudodynamic algorithms is proposed for general pseudodynamic testing. One particular subfamily seems very promising for use in general pseudodynamic testing since the stability problem for a structure does not need to be considered. This is because this subfamily is unconditionally stable for any instantaneous stiffness softening system, linear elastic system and instantaneous stiffness hardening system that might occur in the pseudodynamic testing of a real structure. In addition, it also offers good accuracy when compared to a general second-order accurate method for both linear elastic and nonlinear systems.

Keywords: pseudodynamic test; explicit method; unconditional stability; dominant mode; structural dynamics; instantaneous degree of nonlinearity

1 Introduction

Due to its convenient implementation in testing, an explicit pseudodynamic algorithm (Chang, 1997; Chang, 2000; Chang, 2001; Chang *et al*., 1998; Newmark, 1959; Shing and Mahin, 1987b) is generally preferred over an implicit pseudodynamic algorithm (Chang and Mahin, 1993; Nakashima *et al*., 1990; Shing *et al*., 1991; Thewalt and Mahin, 1995). However, among the currently available integration methods, there are only a few explicit algorithms (Chang, 1997; Chang and Mahin, 1993; Newmark, 1959; Shing and Mahin, 1987b) and most are implicit algorithms (Chang, 1996; Chung and Hulbert, 1993; Hilber *et al*., 1977; Houbolt, 1950; Newmark, 1959; Park, 1975; Wood *et al*., 1981). Although many implicit algorithms are available for step-by-step integration, they were not considered in the early development of the pseudodynamic technique. This is because they involve an iterative procedure in the step-by-step solution of a nonlinear system and it is well known that the behavior of a real specimen is highly path dependent. More recently, some implicit pseudodynamic algorithms have been successfully implemented for use in testing. However, their implementation needs some additional hardware or is more complex (Chang and Mahin, 1993; Nakashima *et al*., 1990; Shing *et al*., 1991; Thewalt and Mahin, 1995) when compared to explicit pseudodynamic algorithms.

The Newmark explicit method (Newmark, 1959) or central difference method is often used to perform pseudodynamic testing. Meanwhile, some explicit pseudodynamic algorithms with acceptable numerical dissipation have been developed to improve the accuracy of the test results since numerical damping can be used to suppress or even eliminate the spurious participation of high frequency responses (Shing and Mahin, 1987b; Chang, 1997; Chang, 2000). However, all the explicit pseudodynamic algorithms are only conditionally stable. Hence, a very small time step might be needed to satisfy the stability limit and thus the critical problem of step displacement control might occur when performing a pseudodynamic test. In order to overcome the conditional stability problem while maintaining the explicitness of each time step, an explicit pseudodynamic algorithm with unconditional stability was proposed by Chang (2002). This algorithm was shown to be unconditionally stable for any instantaneous stiffness softening system and any linear elastic systems, while it can only have conditional stability for an instantaneous stiffness hardening system (Chang, 2007). In this investigation, a new family of explicit algorithms is proposed for the general pseudodynamic testing. In addition, numerical properties and error propagation properties of this family of pseudodynamic algorithms are analytically studied and numerical experiments are used to confirm the analytical predictions. Finally, actual pseudodynamic tests also confirm the feasibility of this family of algorithms.

2 New family of pseudodynamic algorithms

In structural dynamics or earthquake engineering,

Correspondence to: Shuenn-Yih Chang, Department of Civil Engineering, Taipei University of Technology, NTUT Box 2653, No. 1, Section 3, Jungshiau East Road, Taipei 10608, Chinese Taipei
Tel: 886-2-2771-2171 ext 2653; Fax: 886-2-2781-4518
E-mail: changsy@ntut.edu.tw
†Professor; ‡Assistant Professor; §Graduate Student

Supported by: Science Council, Chinese Taipei Under Grant No. NSC-95-2221-E-027-099
Received July 29, 2010; **Accepted** December 23, 2010

the equation of motion for a single degree of freedom (DOF) system is expressed as

$$m\ddot{u} + c\dot{u} + ku = f \tag{1}$$

where m, c, k and f are the mass, viscous damping coefficient, stiffness and external force, respectively; and u, $\dot{u}$ and $\ddot{u}$ are the displacement, velocity and acceleration, respectively.

In performing a pseudodynamic test, the use of an integration method to perform the step-by-step integration is necessary. A family of explicit algorithms is proposed for the pseudodynamic testing and is expressed as

$$\begin{aligned} & ma_{i+1} + cv_{i+1} + kd_{i+1} = f_{i+1} \\ & d_{i+1} = d_i + \beta_1(\Delta t)v_i + \beta_2(\Delta t)^2 a_i \\ & v_{i+1} = v_i + (\Delta t)\left[(1-\gamma)a_i + \gamma a_{i+1}\right] \end{aligned} \tag{2}$$

where

$$\beta_1 = \frac{1 + 2\gamma\xi\Omega_0}{1 + 2\gamma\xi\Omega_0 + \beta\Omega_0^2} \quad , \quad \beta_2 = \frac{\frac{1}{2} - 2\left(\beta - \frac{1}{2}\gamma\right)\xi\Omega_0}{1 + 2\gamma\xi\Omega_0 + \beta\Omega_0^2} \tag{3}$$

where $\Omega_0 = \omega_0(\Delta t)$, and $\omega_0 = \sqrt{k_0/m}$ is the natural frequency of the system determined from the initial stiffness of k_0; ξ is a viscous damping ratio; and β and γ are the parameters governing the numerical properties. Equation (2) reveals that the proposed family algorithm is explicit since the next step displacement d_{i+1} is directly determined from the second line of this equation, which only involves the data of the i-th time step. It is also found that $\beta_2 = \frac{1}{2}\beta_1$ for a zero viscous damping ratio.

Based on the fundamental theory of structural dynamics, $\xi\Omega_0$ and Ω_0^2 can be rewritten in terms of the initial structural properties and the step size. In fact, the relationship of $\xi = c_0/(2m\omega_0)$ and $\Omega_0 = \sqrt{k_0/m}(\Delta t)$ are used. As a result, β_1 and β_2 in Eq. (3) are rewritten as

$$\beta_1 = \frac{1 + \gamma(\Delta t)\left(\frac{c_0}{m}\right)}{1 + \gamma(\Delta t)\left(\frac{c_0}{m}\right) + \beta(\Delta t)^2\left(\frac{k_0}{m}\right)} \quad , \quad \beta_2 = \frac{\frac{1}{2} - \left(\beta - \frac{1}{2}\gamma\right)(\Delta t)\left(\frac{c_0}{m}\right)}{1 + \gamma(\Delta t)\left(\frac{c_0}{m}\right) + \beta(\Delta t)^2\left(\frac{k_0}{m}\right)} \tag{4}$$

where c_0 is introduced to represent an initial viscous damping coefficient and remains invariant for an entire step-by-step integration procedure. It is found that the determinations of the coefficients β_1 and β_2 using Eq. (4) is much easier than Eq. (3) since the expressions of $\xi\Omega_0$ and Ω_0^2 involve solving an eigenvalue problem, which is very time consuming for a multiple DOF system with matrices of larger order. Note that β_1 and β_2 are assumed to be invariant in an entire step-by-step integration procedure.

3 Step-by-step computing procedure

In conducting a pseudodynamic test, the proposed family algorithm can be used to perform the step-by-step integration after determining the coefficients of β_1 and β_2. In order to formulate the step-by-step integration procedure in a matrix form for subsequent analysis, the computing procedure for the (i+1)-th time step is described next.

At first, the displacement d_{i+1} can be calculated from the second line of Eq. (2) since the acceleration, velocity and displacement at the i-th time step are available at the beginning of the (i+1)-th time step. Hence, the restoring force r_{i-1} corresponding to the displacement d_{i+1} can be determined from a mathematically assumed force-displacement relationship and expressed as $r_{i+1} = k_{i+1}d_{i+1}$, where r_{i+1} and k_{i+1} are used to represent the restoring force and stiffness at the end of the (i+1)-th time step. Subsequently, after the substitution of the acceleration a_{i+1}, which can be expressed as a function of v_{i+1} by using the third line of Eq. (2), into the first line of Eq. (2), the velocity at the end of the (i+1)-th time step is found to be

$$v_{i+1} = \left[m + \gamma c(\Delta t)\right]^{-1} \cdot \left[mv_i + (1-\gamma)(\Delta t)ma_i + \frac{\gamma}{m}(\Delta t)\left(f_{i+1} - k_{i+1}d_{i+1}\right)\right] \tag{5}$$

Finally, the first line of Eq. (2) can be used to compute the acceleration a_{i+1}. This computing procedure to obtain d_{i+1}, v_{i+1} and a_{i+1} for the (i+1)-th time step can be written in a recursive matrix form as

$$\boldsymbol{X}_{i+1} = \boldsymbol{A}_{i+1}\boldsymbol{X}_i + \boldsymbol{L}_{i+1}f_{i+1} \tag{6}$$

where $\boldsymbol{X}_{i+1} = \left[d_{i+1} \quad (\Delta t)v_{i+1} \quad (\Delta t)^2 a_{i+1}\right]^{\mathrm{T}}$; $\boldsymbol{A}_{i+1}$ and $\boldsymbol{L}_{i+1}$ are the amplification matrix and the load vector for the (i+1)-th time step, respectively.

4 Numerical properties

In order to realistically reflect the stiffness change in the step-by-step solution of a nonlinear system, the instantaneous degree of nonlinearity δ_{i+1} is defined to be the ratio of the secant stiffness at the end of the (i+1)-th time step over the initial tangent stiffness and is

$$\delta_{i+1} = \frac{k_{i+1}}{k_0} \tag{7}$$

This parameter is used in the subsequent basic analysis and error propagation analysis for the proposed family algorithm. Apparently, $\delta_{i+1} = 1$ implies the instantaneous stiffness at the end of the (i+1)-th time

step is equal to the initial stiffness. Whereas, $\delta_{i+1} > 1$ can be used to represent the case of instantaneous stiffness hardening at the end of the (i+1)-th time step and the case of instantaneous stiffness softening can be represented by $0 < \delta_{i+1} < 1$.

After introducing the instantaneous degree of nonlinearity δ_{i+1} and assuming a zero viscous damping ratio, the explicit expression of the amplification matrix $\boldsymbol{A}_{i+1}$ is found to be

$$\boldsymbol{A}_{i+1}=\begin{bmatrix} 1 & \dfrac{1}{1+\beta\Omega_0^2} & \dfrac{\frac{1}{2}}{1+\beta\Omega_0^2} \\ -\gamma\Omega_{i+1}^2 & 1-\dfrac{\gamma\Omega_{i+1}^2}{1+\beta\Omega_0^2} & 1-\gamma-\dfrac{\frac{1}{2}\gamma\Omega_{i+1}^2}{1+\beta\Omega_0^2} \\ -\Omega_{i+1}^2 & -\dfrac{\Omega_{i+1}^2}{1+\beta\Omega_0^2} & -\dfrac{\frac{1}{2}\Omega_{i+1}^2}{1+\beta\Omega_0^2} \end{bmatrix} \tag{8}$$

The characteristic equation for this matrix can be derived from the equation of $\left|\boldsymbol{A}_{i+1}-\lambda\boldsymbol{I}\right|=0$ and is found to be

$$\lambda^3-A_1\lambda^2+A_2\lambda-A_3=0 \tag{9}$$

where λ is an eigenvalue of the matrix $\boldsymbol{A}_{i+1}$; and the explicit expressions of A_1, A_2 and A_3 are found to be

$$A_1=2-\frac{\left(\gamma+\frac{1}{2}\right)\Omega_{i+1}^2}{1+\beta\Omega_0^2},\quad A_2=1-\frac{\left(\gamma-\frac{1}{2}\right)\Omega_{i+1}^2}{1+\beta\Omega_0^2},\quad A_3=0 \tag{10}$$

Since a linear elastic system is a special case of nonlinear systems, after taking $\Omega_0=\Omega_{i+1}=\Omega$, this equation is reduced to be exactly the same as that of the Newmark family method for linear elastic systems (Hughes, 1987). Therefore, it is implied that the numerical properties of the proposed family algorithm are the same as those of the Newmark family method for linear elastic systems. However, different numerical properties for nonlinear systems may occur, and will be thoroughly explored next.

4.1 Stability

It is manifested from Eq. (9) that the coefficient of $A_3=0$ implies that there is a zero eigenvalue, i.e., $\lambda_3=0$. The third eigenvalue λ_3 is the spurious root since it does not represent a realistic numerical solution of free vibration. Hence, in order to have a bounded oscillatory response, two stability conditions must be satisfied. One is that there are two complex conjugate eigenvalues, and the other is that $\left|\lambda_3\right|<\left|\lambda_{1,2}\right|\le 1$. As a result, these two stability conditions lead to

$$\left(A_1\right)^2-4A_2\le 0,\qquad 0\le A_2\le 1 \tag{11}$$

After substituting Eq. (10) into Eq. (11), the stability conditions for the proposed family algorithm are found to be

$$0<\Omega_0\le\infty \quad \text{if} \quad \beta\ge\tfrac{1}{4}\left(\gamma+\tfrac{1}{2}\right)^2\delta_{i+1} \quad \text{and} \quad \gamma\ge\tfrac{1}{2}$$
$$0<\Omega_0\le\Omega_0^{\mathrm{u}}=\frac{1}{\sqrt{\frac{1}{4}\left(\gamma+\frac{1}{2}\right)^2\delta_{i+1}-\beta}} \quad \text{if} \quad \beta<\tfrac{1}{4}\left(\gamma+\tfrac{1}{2}\right)^2\delta_{i+1} \quad \text{and} \quad \gamma\ge\tfrac{1}{2} \tag{12}$$

where $\Omega_0^{(\mathrm{u})}$ represents the upper stability limit. Equation (12) shows that unconditional stability can be achieved as $\beta\ge\frac{1}{4}\left(\gamma+\frac{1}{2}\right)^2\delta_{i+1}$ and $\gamma\ge\frac{1}{2}$ while the proposed family algorithm only has conditional stability as $\beta<\frac{1}{4}\left(\gamma+\frac{1}{2}\right)^2\delta_{i+1}$ and $\gamma\ge\frac{1}{2}$. Apparently, it is also manifested from this equation that the stability depends upon the instantaneous degree of nonlinearity.

Since the proposed family algorithm has exactly the same characteristic equation as that of the Newmark family method, there is a corresponding member in the proposed family algorithm for any member of the Newmark family method. It is well recognized that the Newmark family method can have at least the second order accuracy for linear elastic systems if $\gamma=\frac{1}{2}$ is chosen (Belytschko and Hughes, 1983). Since integration methods with the second order accuracy are of interest in practice, some well-known members in the subfamily of the Newmark family method with $\gamma=\frac{1}{2}$ and its corresponding members in the proposed family algorithm are listed in Table 1 for comparison. Note that the unconditional stability range increases as the value of β increases. M1 is the Newmark explicit method. Since M2 and M3 can only have unconditional stability in the range of $\delta_{i+1}\le\frac{1}{3}$ and $\delta_{i+1}\le\frac{2}{3}$, respectively, their general applications are very limited. Whereas, M4 to M7 seem promising from a stability point of view since they have unconditional stability for any instantaneous stiffness softening systems and linear elastic systems. It is very interesting to find that M5 to M7 can have unconditional stability for instantaneous stiffness hardening systems in a given range, in addition to any instantaneous stiffness softening systems and any linear elastic systems. In order to gain an insight into the stability properties of the proposed family algorithms, Eq. (12) is plotted

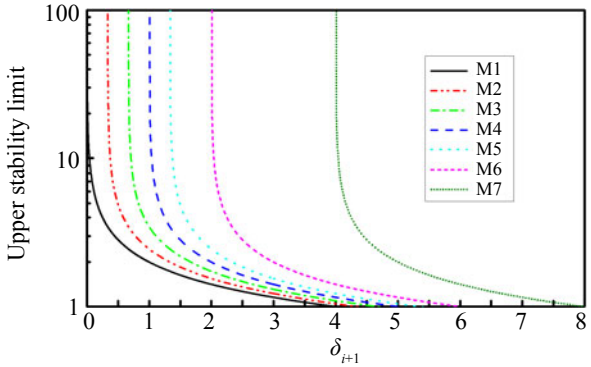

Fig. 1 Variation of upper stability limit with δ_{i+1} for proposed family algorithm

in Fig. 1. Each curve decreases from infinity to zero as δ_{i+1} increases from a certain value to infinity. For example, the upper stability limit is infinity in the range of $\delta_{i+1} \le 1$ for M4, and it decreases from infinity to zero as δ_{i+1} increases from 1 to infinity. Note that M4 has been previously published (Chang, 2002; Chang, 2007). Apparently, there is no unconditional stability range for M1, i.e., the Newmark explicit method.

4.2 Accuracy verification

In order to evaluate the period distortion of the proposed family algorithm introduced at the $(i+1)$-th time step, the two complex conjugate eigenvalues of the characteristic equation can be expressed in an exponential form as

$$\lambda_{1,2} = \frac{1}{2}A_1 \pm \mathrm{j}\sqrt{A_2 - \frac{1}{4}A_1^2} = \mathrm{e}^{-\bar{\xi}\bar{\Omega}_{i+1} \pm \mathrm{j}\bar{\Omega}_{i+1}} \tag{13}$$

where $\mathrm{j} = \sqrt{-1}$ and $\bar{\Omega}_{i+1} = \bar{\omega}_{i+1}(\Delta t)$. This expression can be applied to determine the phase shift of $\bar{\Omega}_{i+1}$ and the numerical damping ratio of $\bar{\xi}_{i+1}$ at the $(i+1)$-th time step. As a result, they can be computed by

$$\bar{\Omega}_{i+1} = \arctan\sqrt{\frac{4A_2}{A_1^2} - 1}, \qquad \bar{\xi}_{i+1} = -\frac{\ln(A_2)}{2\bar{\Omega}_{i+1}} \tag{14}$$

where $\bar{\xi}_{i+1}$ is a measure of numerical dissipation. The relative period error is often used to measure period distortion and is defined as

$$P_{i+1} = \frac{\bar{T}_{i+1} - T_{i+1}}{T_{i+1}} = \frac{\omega_{i+1}}{\bar{\omega}_{i+1}} - 1 \tag{15}$$

where $\bar{T}_{i+1} = (2\pi)/\bar{\omega}_{i+1}$ and $T_{i+1} = (2\pi)/\omega_{i+1}$ are used to represent the computed and true periods of the system, respectively. In general, $\bar{\xi}_{i+1}$ and $\bar{\omega}_{i+1}$ are considered as the quantities corresponding to ξ_{i+1} and ω_{i+1} in a numerical solution.

Using Eq. (14) with the coefficients of A_1, A_2 and A_3 found in Eq. (10), it is very straightforward to find that $\bar{\xi}_{i+1} = 0$ for M1 to M7. This is because $\gamma = \frac{1}{2}$ was adopted for M1 to M7 and thus leads to A_2=1, which implies that there is a zero numerical damping ratio if Eq. (14) is applied.

Figure 2 shows the variations of relative period errors with $\Delta t/T_0$ for δ_{i+1}= 0.5, 1 , 1.5 and 2 for the seven members of the proposed family algorithm listed in Table 1. In general, the absolute relative period error increases as $\Delta t/T_0$ increases as δ_{i+1} and β are given. In Fig. 2(a), the case of instantaneous stiffness softening is considered, where M1 shows period shrinkage while period elongation is found for the rest of the members. In Fig. 2(b), the case of instantaneous stiffness invariant is considered, where the period is shrunk for M1 and M2; and the relative period error is almost zero for M2 as δ_{i+1}=1. This is because for linear elastic systems, M2 has a third order accuracy for a linear elastic system. Both Figs. 2(c) and 2(d) consider the case of instantaneous stiffness hardening. In Fig. 2(c), M1 and M2 lead to period shrinkage while M3 to M7 results in period elongation. Meanwhile, the period is shortened in Fig. 2(d) for M1 to M3 and the rest of the members show period elongation. It is important to note that M2 has a third order accuracy for linear elastic systems; and for nonlinear systems, its accuracy reduces to be roughly the same as the other second-order accurate algorithms.

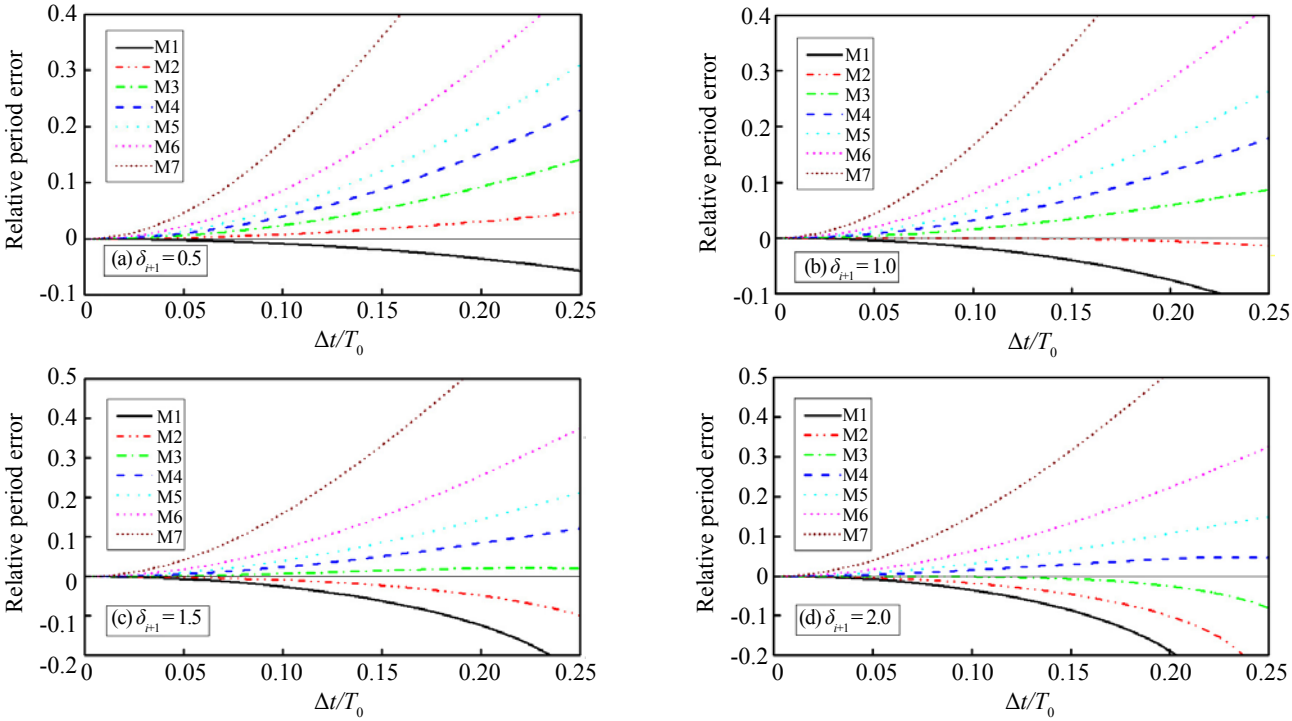

Fig. 2 Variations of relative period errors with $\Delta t/T_0$ for different δ_{i+1}

In each plot of Fig. 2, the relative period error of each algorithm seems negligible as $\Delta t / T_0 \leq 0.05$ except that M7 shows more significant period distortion. Thus, these members of the proposed family algorithm except for M7 can provide a reliable solution with comparable accuracy for nonlinear systems, if the condition $\Delta t / T_0 \leq 0.05$ is met for the modes of interest. This may be considered as a rough guideline for selecting an appropriate time step.

As a summary of this numerical property study, it seems that M1 to M3 are of no interest for practical applications since they cannot have unconditional stability for any instantaneous stiffness systems, which are very commonly experienced in structural dynamics or earthquake engineering. Although M7 has the best stability property, its very significant period distortion might greatly limit its application. Hence, M4 to M6 are the most significant in this study.

5 Error propagation properties

Error propagation analysis of a pseudodynamic algorithm is generally needed in its developing stage (Peek and Yi, 1990a; Peek and Yi, 1990b; Shing and Mahin, 1987a; Shing and Mahin, 1990; Shing and Manivannan, 1990). In the following error propagation analysis, a general nonlinear system is considered and the evaluation technique proposed by Chang (2003 and 2005) is used. To mathematically model the error propagation procedure in the pseudodynamic testing of a nonlinear system, the following notations are defined.

d_i = exact numerically computed displacement at step i without errors.

d_i^{e} = exact displacement at step i, including the effects of errors at previous steps.

d_i^{a} = actual displacement at step i, including the effects of previous errors and errors introduced at the current step.

r_i = exact numerically computed restoring force at step i without errors.

r_i^{e} = exact restoring force at step i, including the effects of errors at previous steps.

r_i^{a} = actual restoring force at step i, including the effects of previous errors and errors introduced at the current step.

e_i^{d} = displacement error introduced at step i.

e_i^{r} = force error introduced at step i.

5.1 Error propagation equation

By using the above notations, the following relationships can be formulated:

$$\begin{aligned} d_{i+1}^{\mathrm{a}} &= d_{i+1}^{\mathrm{e}} + e_{i+1}^{\mathrm{d}} \\ r_{i+1}^{\mathrm{a}} &= r_{i+1}^{\mathrm{e}} + e_{i+1}^{\mathrm{r}} \end{aligned} \tag{16}$$

where the restoring force error e_{i+1}^{r} can be further expressed as

$$e_{i+1}^{\mathrm{r}} = k_{i+1} e_{i+1}^{\mathrm{rd}} \tag{17}$$

where e_{i+1}^{rd} is the amount of displacement error corresponding to the restoring force error e_{i+1}^{r} at the (i+1)-th time step. Using the actual displacement and actual restoring force as shown in Eq. (16), which includes the current step errors e_{i+1}^{d} and e_{i+1}^{r}, Eq. (6) can be reformulated as follows

$$\boldsymbol{X}_{i+1}^{\mathrm{e}} = \boldsymbol{A}_{i+1} \boldsymbol{X}_i^{\mathrm{e}} + \boldsymbol{L}_{i+1} f_{i+1} + \boldsymbol{M}_{i+1} e_i^{\mathrm{d}} - \boldsymbol{N}_{i+1} e_{i+1}^{\mathrm{rd}} \tag{18}$$

where $\boldsymbol{X}_{i+1}^{\mathrm{e}} = \left[d_{i+1}^{\mathrm{e}},\ (\Delta t) v_{i+1}^{\mathrm{e}},\ (\Delta t)^2 a_{i+1}^{\mathrm{e}} \right]^{\mathrm{T}}$ is defined; and the vectors $\boldsymbol{M}_{i+1}$ and $\boldsymbol{N}_{i+1}$ corresponding to e_i^{d} and e_{i+1}^{rd} are found to be

$$\boldsymbol{M}_{i+1} = \begin{bmatrix} 1 \\ -\frac{1}{2}\Omega_{i+1}^2 \\ -\Omega_{i+1}^2 \end{bmatrix} \quad , \quad \boldsymbol{N}_{i+1} = \begin{bmatrix} 0 \\ \frac{1}{2}\Omega_{i+1}^2 \\ \Omega_{i+1}^2 \end{bmatrix} \tag{19}$$

Subtracting Eq. (6) from Eq. (18) yields the error propagation equation:

$$\boldsymbol{\varepsilon}_{i+1} = \boldsymbol{A}_{i+1} \boldsymbol{\varepsilon}_i + \boldsymbol{M}_{i+1} e_i^{\mathrm{d}} - \boldsymbol{N}_{i+1} e_{i+1}^{\mathrm{rd}} \tag{20}$$

where the error cumulative vector $\boldsymbol{\varepsilon}_{i+1}$ for the (i+1)-th time step is defined as $\boldsymbol{\varepsilon}_{i+1} = \boldsymbol{X}_{i+1}^{\mathrm{e}} - \boldsymbol{X}_{i+1}$ and can be explicitly expressed as

$$\boldsymbol{\varepsilon}_{i+1} = \begin{bmatrix} \varepsilon_{i+1}^{(1)} \\ \varepsilon_{i+1}^{(2)} \\ \varepsilon_{i+1}^{(3)} \end{bmatrix} = \begin{bmatrix} d_{i+1}^{\mathrm{e}} - d_{i+1} \\ (\Delta t)\left(v_{i+1}^{\mathrm{e}} - v_{i+1} \right) \\ (\Delta t)^2 \left(a_{i+1}^{\mathrm{e}} - a_{i+1} \right) \end{bmatrix} \tag{21}$$

Note that $\varepsilon_{i+1}^{(1)} = e_{i+1}^{\mathrm{d}}$ and is the cumulative displacement error for the (i+1)-th time step.

The amplification matrix of $\boldsymbol{A}_{i+1}$ and the vectors of $\boldsymbol{M}_{i+1}$ and $\boldsymbol{N}_{i+1}$ might vary for each time step for a nonlinear system. Hence, in this study, the error propagation analysis of a nonlinear system is conducted for a few consecutive time steps but not for an entire pseudodynamic test procedure. However, it still provides valuable information for a pseudodynamic algorithm. For this purpose, the pseudodynamic error propagated from the previous one and two time steps to the current time step is mathematically derived next. At first, after repeated substitutions of $\boldsymbol{\varepsilon}_{i-1}$ and $\boldsymbol{\varepsilon}_i$ into $\boldsymbol{\varepsilon}_{i+1}$ through Eq. (20), the cumulative equation is formulated as:

$$\begin{aligned} \boldsymbol{\varepsilon}_{i+1} &= \boldsymbol{\varepsilon}_{i+1}^{(d)} - \boldsymbol{\varepsilon}_{i+1}^{(r)} \\ \boldsymbol{\varepsilon}_{i+1}^{(\mathrm{d})} &= \boldsymbol{A}_{i+1} \boldsymbol{A}_i \boldsymbol{M}_{i-1} e_{i-2}^{\mathrm{d}} + \boldsymbol{A}_{i+1} \boldsymbol{M}_i e_{i-1}^{\mathrm{d}} + \boldsymbol{M}_{i+1} e_i^{\mathrm{d}} \\ \boldsymbol{\varepsilon}_{i+1}^{(\mathrm{r})} &= \boldsymbol{A}_{i+1} \boldsymbol{A}_i \boldsymbol{N}_{i-1} e_{i-1}^{\mathrm{rd}} + \boldsymbol{A}_{i+1} \boldsymbol{N}_i e_i^{\mathrm{rd}} + \boldsymbol{N}_{i+1} e_{i+1}^{\mathrm{rd}} \end{aligned} \tag{22}$$

The cumulative error vector $\boldsymbol{\varepsilon}_{i+1}$ consists of $\boldsymbol{\varepsilon}_{i+1}^{(\mathrm{d})}$ and $\boldsymbol{\varepsilon}_{i+1}^{(\mathrm{r})}$, where $\boldsymbol{\varepsilon}_{i+1}^{(\mathrm{d})}$ is the error vector caused by displacement

feedback errors and $\boldsymbol{\varepsilon}_{i+1}^{(\mathrm{r})}$ is caused by restoring force feedback errors.

Substituting $\boldsymbol{A}_k$, for $k = i$ and i+1, and $\boldsymbol{M}_k$ and $\boldsymbol{N}_k$, for $k = i$–1, i and i+1, into Eq. (22), yields the cumulative displacement error at the (i+1) time step:

$$e_{i+1}^{\mathrm{d}} = \left(D_i e_i^{\mathrm{d}} + D_{i-1} e_{i-1}^{\mathrm{d}} + D_{i-2} e_{i-2}^{\mathrm{d}}\right) - \left(R_i e_i^{\mathrm{rd}} + R_{i-1} e_{i-1}^{\mathrm{rd}}\right) \quad (23)$$

where

$$D_i = 1,\ D_{i-1} = \frac{1+\beta\Omega_0^2 - \Omega_i^2}{1+\beta\Omega_0^2},$$
$$D_{i-2} = 1 - \frac{2\Omega_{i-1}^2 + \Omega_i^2}{1+\beta\Omega_0^2} + \frac{\Omega_{i-1}^2\Omega_i^2}{\left(1+\beta\Omega_0^2\right)^2} \quad (24)$$

and

$$R_i = \frac{\Omega_i^2}{1+\beta\Omega_0^2},\quad R_{i-1} = \frac{2\Omega_{i-1}^2}{1+\beta\Omega_0^2} - \frac{\Omega_{i-1}^2\Omega_i^2}{\left(1+\beta\Omega_0^2\right)^2} \quad (25)$$

Using the same evaluation technique proposed by Chang (2003 and 2005), Eq. (23) can be rewritten in the following form

$$e_{i+1}^{\mathrm{d}} = E^{(\mathrm{d})} \sum_{k=i}^{i-1} \cos\left[(i-k)\bar{\Omega}_{i+1} + \alpha_{i+1}\right] e_k^{\mathrm{d}} + D_{i-2} e_{i-2}^{\mathrm{d}} -$$
$$E^{(\mathrm{r})} \sum_{k=i}^{i-1} \sin\left[(i-k)\bar{\Omega}_{i+1} + \beta_{i+1}\right] e_k^{\mathrm{rd}} \quad (26)$$

where α_{i+1} and β_{i+1} are phase angles; and the explicit expressions of $E^{(\mathrm{d})}$ and $E^{(\mathrm{r})}$ are found to be

$$E^{(\mathrm{d})} = \sqrt{1 + \frac{\left(\frac{1}{2}\Omega_{i+1}^2 - \Omega_i^2\right)^2}{\Omega_{i+1}^2\left(1+\beta\Omega_0^2 - \frac{1}{4}\Omega_{i+1}^2\right)}}$$
$$E^{(\mathrm{r})} = \sqrt{\left(\frac{\Omega_i^2}{1+\beta\Omega_0^2}\right)^2 + \frac{\left[2\Omega_{i-1}^2\left(1+\beta\Omega_0^2 - \frac{1}{2}\Omega_i^2\right) - \Omega_i^2\left(1+\beta\Omega_0^2 - \frac{1}{2}\Omega_{i+1}^2\right)\right]^2}{\Omega_{i+1}^2\left(1+\beta\Omega_0^2\right)^2\left(1+\beta\Omega_0^2 - \frac{1}{4}\Omega_{i+1}^2\right)}} \quad (27)$$

where $E^{(\mathrm{d})}$ and $E^{(\mathrm{r})}$ are the error amplification factors for the displacement and restoring force feedback errors from the previous one and two time steps to the cumulative displacement error e_{i+1}^{d} for the current time step.

5.2 Characteristics of error propagation equation

Equation (23) shows that the error contribution from the displacement feedback errors e_i^{d} and e_{i-1}^{d} to the cumulative displacement error e_{i+1}^{d} depends upon the error amplification factor of $E^{(\mathrm{d})}$. Whereas, the error contribution from the restoring force feedback errors e_i^{rd} and e_{i-1}^{rd} to the cumulative displacement error e_{i+1}^{d} is dependent upon the error amplification factor of $E^{(\mathrm{r})}$. Thus, the error propagation characteristics of the proposed family algorithm can be revealed by plotting Eq. (24). For this purpose, three cases of different values of δ_{i-1}, δ_i and δ_{i+1} are considered and are chosen to be

$$\text{Case A} \qquad \delta_{i-1} = \delta_i = \delta_{i+1} = 0.75$$

for instantaneous stiffness softening

$$\text{Case B} \qquad \delta_{i-1} = \delta_i = \delta_{i+1} = 1.00 \quad (28)$$

for instantaneous stiffness invariant

$$\text{Case C} \qquad \delta_{i-1} = \delta_i = \delta_{i+1} = 1.25$$

for instantaneous stiffness hardening

Variations of $E^{(\mathrm{d})}$ and $E^{(\mathrm{r})}$ with Ω_0 are shown in Figs. 3 and 4, respectively. Note that the error amplification factor $E^{(\mathrm{d})}$ increases with the instantaneous degree of nonlinearity for a specified Ω_0 for the four members of the proposed family algorithm and it tends to infinity as its upper stability limit is approached. However, for the Case A of M4 and all the three cases of M5 and M6, each curve increases gradually from 1 to a larger value and then seemingly levels up as Ω_0 increases from 0 to 10. On the other hand, the error amplification factor $E^{(d)}$ increases as the β value decreases for a given case with a given Ω_0. This implies that M1 has the worst error propagation properties for the displacement feedback error while M6 has the best error propagation properties, among the four members. Very similar phenomena can also be observed from Fig. 4 except that the error amplification factor $E^{(\mathrm{r})}$ no longer starts from 1 but instead begins near its origin.

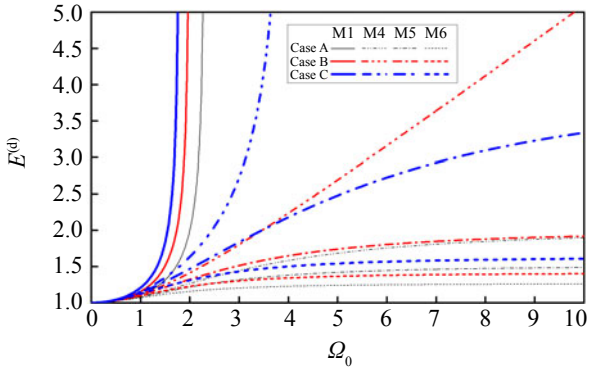

Fig. 3 Error amplification factor for displacement feedback error

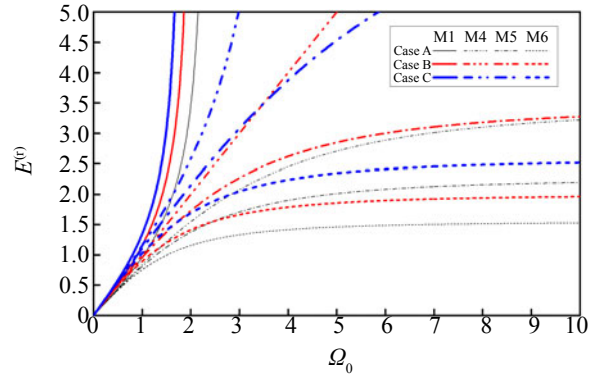

Fig. 4 Error amplification factor for restoring force feedback error

6 General pseudodynamic testing

After investigating the numerical and error propagation properties of the proposed family algorithm in the pseudodynamic testing of a nonlinear system, it is found that some members of the subfamily of $\gamma = \frac{1}{2}$ seem very promising for use in general pseudodynamic testing. This is concluded after the cautious considerations of implementation, stability, accuracy and error propagation.

Due to the explicitness of each time step, any member of the proposed family algorithm can have an explicit implementation when performing a pseudodynamic test. In fact, any member of this family can be implemented to be the same as that of the Newmark explicit method except that it is especially necessary to determine the constant coefficients as shown in Eq. (4). For the proposed family algorithm, it is found that the larger the β value, the more likely it is that the unconditional stability is $\gamma = \frac{1}{2}$. This implies that a member with a large value of β is preferred based on stability consideration. However, based on accuracy consideration, Fig. 2 reveals that a large β value will lead to a more significant period distortion. Hence, after considering stability and accuracy, M5 and M6 might be selected for the general pseudodynamic testing. This is explained as follows. In practical applications, it is very rare to experience a test specimen whose instantaneous stiffness hardening property can be as large as $\delta_{i+1} > \frac{4}{3}$ or $\delta_{i+1} > 2$. Hence, there is no need to worry about the stability problem if M5 or M6 is applied to perform a general pseudodynamic test. Furthermore, both members can have commensurate period distortion as the Newmark explicit method for a small value of $\Delta t / T_0$, say $\Delta t / T_0 \leq 0.05$. On the other hand, error propagation analysis reveals that error amplification factors of displacement feedback error $E^{(d)}$ and restoring force feedback factor $E^{(r)}$ decrease as the β value increases for a given Ω_0 and converge to specific limited values for a large value of Ω_0 within the unconditional stability range. Thus, M5 and M6 are also preferred due to less error propagation when compared to the other members except for M7.

In this study, only some specific members of the proposed family algorithm are considered for illustration purposes, such as the members shown in Table 1. However, it is clear that members with a β value in the range of $\frac{1}{3} \leq \beta \leq \frac{1}{2}$ or $\frac{1}{3} \leq \beta \leq \frac{2}{3}$ and $\gamma = \frac{1}{2}$ of the proposed family algorithm are also promising for use in the general pseudodynamic testing, not only the members of M5 and M6. The most important characteristic of these members is that they are unconditionally stable for a certain range of instantaneous stiffness hardening, which might be actually experienced in the pseudodynamic testing of an actual structure, in addition to any linear elastic systems and any instantaneous stiffness softening systems. As a result, there is no need to consider the stability problem in practice.

7 Implementation for an MDOF system

It is shown that the numerical properties of the proposed family algorithm are the same as those of the Newmark family method for linear elastic systems. However, drastic differences in numerical properties for nonlinear systems are found between these two families. Therefore, it is important to examine the performance of the proposed family algorithm in the solution of a nonlinear system and in performing a pseudodynamic test. For this purpose, it is implemented for a MDOF system, and can be expressed as

$$\begin{aligned} &\boldsymbol{M}\boldsymbol{a}_{i+1} + \boldsymbol{C}_0\boldsymbol{v}_{i+1} + \boldsymbol{r}_{i+1} = \boldsymbol{f}_{i+1} \\ &\boldsymbol{d}_{i+1} = \boldsymbol{d}_i + \beta_1(\Delta t)\boldsymbol{v}_i + \beta_2(\Delta t)^2\boldsymbol{a}_i \\ &\boldsymbol{v}_{i+1} = \boldsymbol{v}_i + (\Delta t)\left[(1-\gamma)\boldsymbol{a}_i + \gamma\boldsymbol{a}_{i+1}\right] \end{aligned} \tag{29}$$

where $\boldsymbol{C}_0$ is the initial damping coefficient matrix and is generally determined from the initial structural properties; the restoring force vector can be expressed $\boldsymbol{r}_{i+1} = \boldsymbol{K}_{i+1}\boldsymbol{d}_{i+1}$, and $\boldsymbol{K}_{i+1}$ is the stiffness matrix at the end of the (i+1)-th time step. Note that the stiffness matrix is not determined during a pseudodynamic test. The coefficients become

$$\begin{aligned} \beta_1 &= \left[\boldsymbol{I} + \gamma(\Delta t)\boldsymbol{M}^{-1}\boldsymbol{C}_0 + \beta(\Delta t)^2\boldsymbol{M}^{-1}\boldsymbol{K}_0\right]^{-1} \cdot \\ &\quad \left[\boldsymbol{I} + \gamma(\Delta t)\boldsymbol{M}^{-1}\boldsymbol{C}_0\right] \\ \beta_2 &= \left[\boldsymbol{I} + \gamma(\Delta t)\boldsymbol{M}^{-1}\boldsymbol{C}_0 + \beta(\Delta t)^2\boldsymbol{M}^{-1}\boldsymbol{K}_0\right]^{-1} \cdot \\ &\quad \left[\frac{1}{2}\boldsymbol{I} - \left(\beta - \frac{1}{2}\gamma\right)(\Delta t)\boldsymbol{M}^{-1}\boldsymbol{C}_0\right] \end{aligned} \tag{30}$$

where $\boldsymbol{K}_0$ is the initial stiffness matrix. Since the coefficient matrices of β_1 and β_2 must be determined before performing a pseudodynamic test, it is necessary to obtain the initial stiffness matrix. This initial stiffness matrix can be experimentally obtained by the direct stiffness method. This method imposes a unit displacement for the specified DOF by using a hydraulic actuator, and then the restoring forces developed by the specimen in each DOF are measured by load cells. As a result, these restoring forces provide the stiffness coefficients of the correspondent column. This procedure can be repeated until the initial stiffness is achieved.

In performing a pseudodynamic test, the second line of Eq. (29) is applied to calculate the displacement vector, and subsequently servo-hydraulic actuators are used to impose the computed displacement vector upon the test specimen. After measuring the restoring force vector through load cells, the acceleration vector can be expressed in terms of $\boldsymbol{r}_{i+1}$ and $\boldsymbol{v}_{i+1}$ by using the first line of Eq. (29). Hence, substituting this result into the third

line of Eq. (29) yields the velocity vector:

$$\boldsymbol{v}_{i+1}=\left[\boldsymbol{M}+\gamma(\Delta t)\boldsymbol{C}_0\right]^{-1}\cdot \left\{\boldsymbol{M}\left[\boldsymbol{v}_i+(1-\gamma)(\Delta t)\boldsymbol{a}_i\right]+\gamma(\Delta t)\left(\boldsymbol{f}_{i+1}-\boldsymbol{r}_{i+1}\right)\right\} \quad (31)$$

Finally, the acceleration vector can be calculated by using the equation of motion, i.e., the first line of Eq. (29).

8 Numerical examples

To confirm the analytically determined numerical properties of the proposed family algorithm for both linear elastic and nonlinear systems, some numerical examples are illustrated. In particular, the stability problem and the use of the rough guideline $\Delta t/T_0 \le 0.05$ to select an appropriate time step for the step-by-step integration are addressed. In the following numerical study, a two-story shear building is considered and the stiffness for each story is assumed to be in the form of

$$k=k_0\left[1+\alpha\sqrt{|\Delta u|}\right] \quad (32)$$

where k_0 is the initial stiffness and Δu is a interstory drift. Apparently, the structural nonlinearity arises from the interstory drift if $\alpha \neq 0$ is chosen. The case of instantaneous stiffness softening can be simulated if $\alpha<0$ is chosen while $\alpha>0$ can be used to mimic the case of instantaneous stiffness hardening.

The lumped mass for the bottom story is taken to be $m_1=10^3$ kg while that for the top story is taken as $m_2=6\times10^3$ kg. In order to confirm the correctness of the above analytically obtained numerical properties for general nonlinear systems, three structural systems with different stiffness types are considered. The stiffness types include instantaneous stiffness softening, invariant and hardening. In general, the initial stiffness is chosen to be $k_{0\text{-}1}=10^7$ N/m and $k_{0\text{-}2}=10^5$ N/m for the bottom and top stories, respectively. Hence, the three systems with different stiffness types can be simulated by taking different coefficients of α for the nonlinear term.

Sys-1 $\alpha_1=0$ $\alpha_2=0$
instantaneous stiffness invariant system

Sys-2 $\alpha_1=-0.1$ $\alpha_2=-0.2$
instantaneous stiffness softening system

Sys-3 $\alpha_1=1$ $\alpha_2=2$
instantaneous stiffness hardening system

where α_1 and α_2 are the constant coefficients of the nonlinear stiffness terms for the bottom and top stories, respectively. The natural frequencies of the structure are found to be 4.06 and 100.5 rad/s based on the initial stiffness matrix. This structure is excited by a ground acceleration of 20sin(t) at its base. For the three systems, the numerical result of each system obtained from the Newmark explicit method (i.e., M1) with Δt = 0.0001 s is considered as an "exact" solution for comparison. Meanwhile, M1 with Δt = 0.02 s, and M4, M5 and M6 with Δt = 0.07 s are also used to compute numerical solutions.

8.1 Example 1 — Sys-1

It is clear that Sys-1 is a linear elastic system, and its numerical solutions are shown in Fig. 5. Note that the results for M1 with Δt = 0.02s become unstable in the early response while those for M4, M5 and M6 with Δt = 0.07 s are reliable. Apparently, the instability that occurred in M1 is due to the violation of the upper stability limit for the second mode since for Δt = 0.02 s, the value of $\Omega_0^{(2)}$ is as large as 2.01, which is slightly larger than the upper stability limit of 2. Unconditional stability is indicated by the results for M4, M5 and M6 with Δt = 0.07 s since it remains stable for the value of $\Omega_0^{(2)}$ as large as 7.04 for the second mode. The response contribution from the second mode to the total response is insignificant since reliable solutions can be obtained for M4, M5 and M6 with Δt = 0.07 s, where the first mode is reliably integrated while a very significant period distortion is found in the second mode. This is because $\Delta t/T_0^{(1)}=\frac{1}{22}$ for the first mode and $\Delta t/T_0^{(2)}=1.12$ for the second mode. Note that $\Delta t/T_0^{(1)}=\frac{1}{22}$ is close to the rough guideline of $\Delta t/T_0<0.05$ for the mode of interest. Hence, the first mode is reliably integrated for M4, M5 and M6.

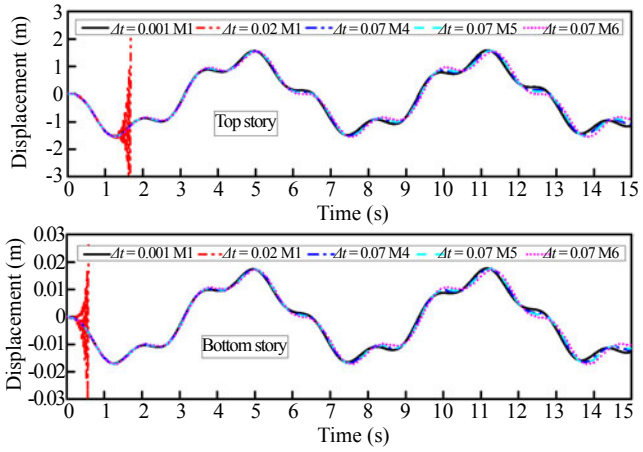

Fig. 5 Displacement response time histories for Sys-1

8.2 Example 2 — Sys-2

Figure 6 shows the displacement responses for Sys-2. In addition, the response time histories of relative period error, instantaneous degree of nonlinearity and upper stability limit are plotted in Fig. 7. Note that reliable solutions are obtained for M4, M5 and M6 with Δt = 0.07 s since the relative period error is small

for the first mode, as shown in Fig. 7(a), although the second mode shows a very significant period distortion, as shown in Fig. 7(b). Figures 7(c) and 7(d) reveal that the instantaneous degree of nonlinearity of both modes are always less than or equal to 1, i.e., in the ranges of $0.7 \le \delta_i^{(1)} \le 1$ and $0.98 \le \delta_i^{(2)} \le 1$. Therefore, a stable computation can be achieved for M4, M5 and M6 since they behave in an unconditional stability state for any instantaneous stiffness softening system. It is interesting to find that the top story response of M1 with $\Delta t = 0.02$ s is accurate while the bottom story response shows very significant high frequency fluctuation with respect to the exact solution. This might be due to the slight violation of the upper stability limit for the second mode at the beginning of the motion while the stability is regained after the stiffness is softening. Note that there is no

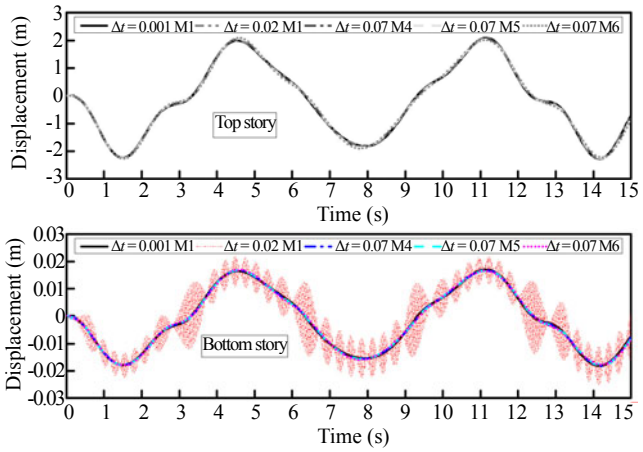

Fig. 6 Displacement response time histories for Sys-2

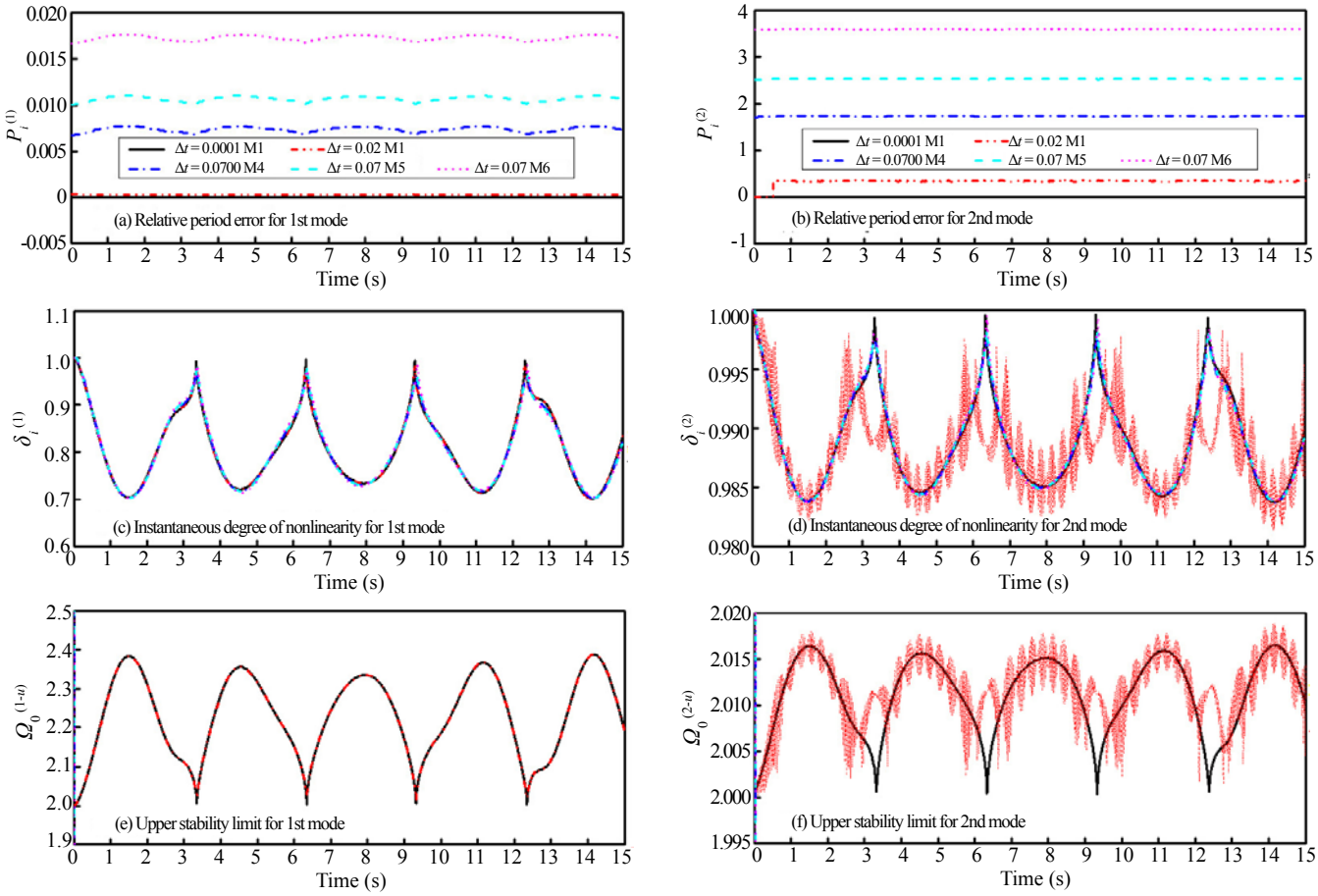

Fig. 7 Response time histories for Sys-2

significant high frequency fluctuation with respect to the exact solution for the top story, since the response contribution from the second mode to the top story response is insignificant.

8.3 Example 3 — Sys-3

Analytical results reveal that M4, M5 and M6 will become conditionally stable as $\delta_{i+1}>1$, $\frac{4}{3}$ and 2, respectively. Hence, it is of great interest to explore their performance in the solution of an instantaneous stiffness hardening system. As a result, the displacement responses for Sys-3 are shown in Fig. 8 and the response time histories of relative period error, instantaneous degree of nonlinearity and upper stability limit are

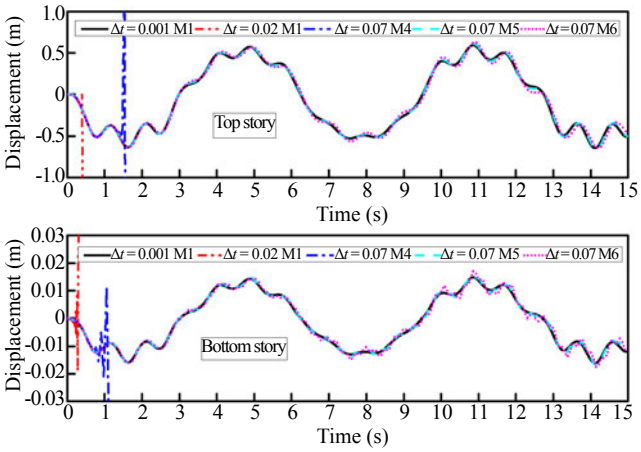

Fig. 8 Displacement response time histories for Sys-3

plotted in Fig. 9. Figure 8 shows that for both M5 and M6 with $\Delta t = 0.07$ s, the results are acceptable; while for M1 with $\Delta t = 0.02$ s and M4 with $\Delta t = 0.07$ s, numerical instability occurs. This might be explained by Fig. 9. The system experiences instantaneous stiffness hardening since $\delta_i^{(1)} \geq 1$ and $\delta_i^{(2)} \geq 1$ are found from Figs. 9(c) and 9(d) for both modes. Thus, the upper stability limit for M1 is shrunk and the use of $\Delta t = 0.02$s lead to instability due to the violation of the upper stability limit as shown in Figs. 9(e) and 9(f). A similar phenomenon is found for M4 with $\Delta t = 0.07$ s. It is apparent that a stable computation is responsible for M5 and M6 achieving reliable solutions since the conditional stability limits are satisfied. This is manifested from Figs. 9(c) and 9(e).

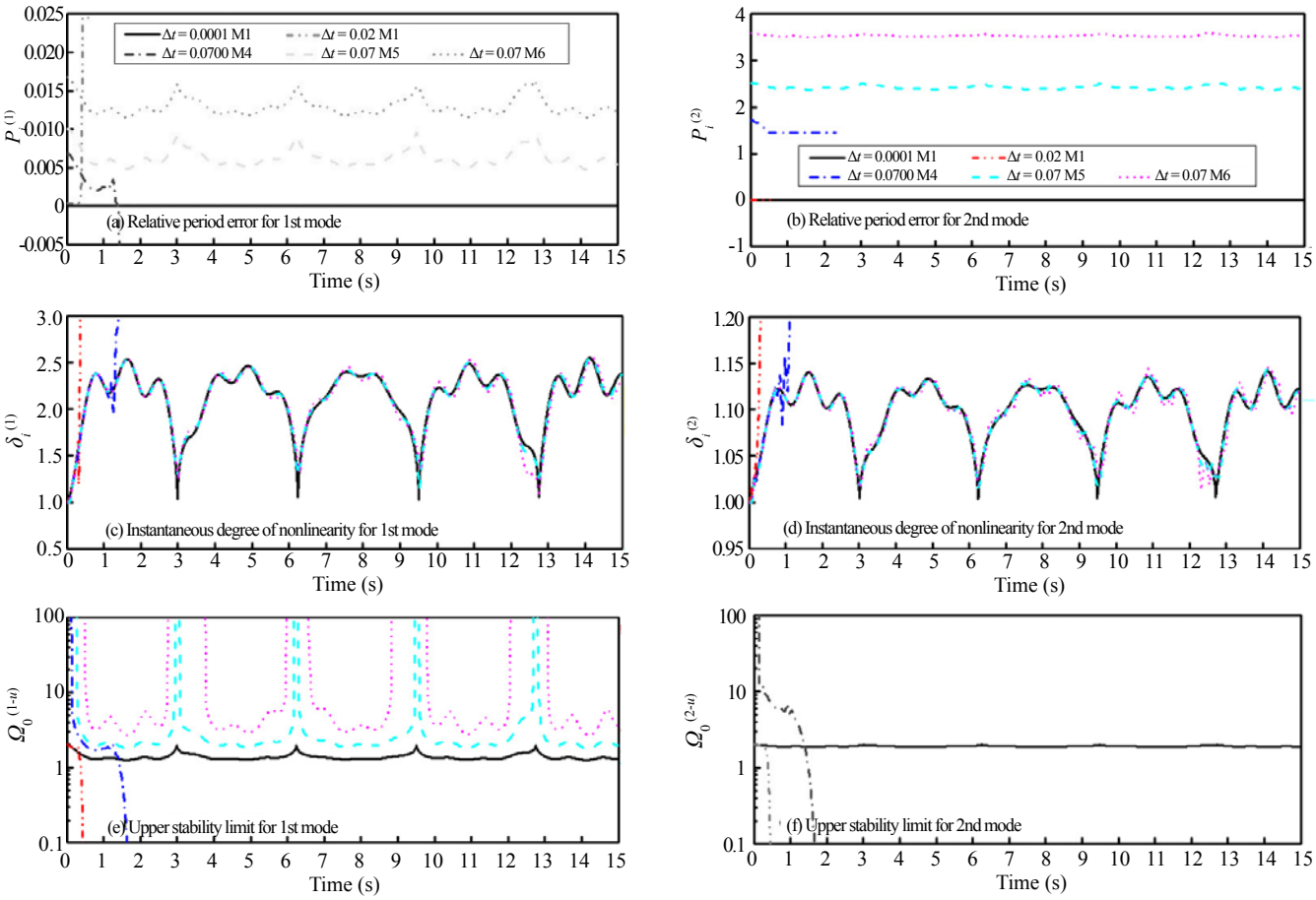

Fig. 9 Response time histories for Sys-3

9 Numerical simulations

To numerically illustrate that the subfamily of the proposed family algorithm, whose β value is selected to be in the range of $\frac{1}{3} \leq \beta \leq \frac{1}{2}$ or $\frac{1}{3} \leq \beta \leq \frac{2}{3}$ and $\gamma = \frac{1}{2}$, such as M5 and M6, have better error propagation properties than those of the currently available explicit pseudodynamic algorithms, a series of computer simulations of the pseudodynamic tests are studied next. In these numerical simulations, the displacement error introduced into the imposed displacement in each DOF per time step is considered as a random variable, whose distribution is assumed to be a truncated normal distribution. Simulation details can be found in Chang SY (2002) and are not elaborated here. In order to simulate a properly adjusted test, the mean value of the truncated normal distribution is taken to be zero. In addition, its standard deviation is assumed to be 1/3 of

the tolerance limit, which is taken to be 0.2 mm in all numerical simulations. This implies that the random error simulated in each time step might be as large as 0.2 mm.

The structural systems of Sys-1, Sys-2 and Sys-3 subjected to the same ground acceleration of 20sin(t) at their base were also adopted for computer simulations. Simulation results for the bottom story are plotted in Figs. 10 to 12 for Sys-1, Sys-2 and Sys-3, respectively. Since the displacement responses of the top story are much larger than the simulation errors introduced into the computed displacements, they are almost unaffected by these simulation errors and thus the response time histories of the top story will not be discussed here. The solution for M4 with a time step of Δt = 0.0001 s is considered as an exact solution for comparison. Note that no simulation errors are introduced into the system to obtain the exact solution. M4, M5 and M6 with a time step of Δt = 0.07 s are used to perform the computer simulations where the simulated errors are introduced into each DOF per time step. In each figure, the top plot shows the displacement response time histories while the time histories of cumulative error and step error are shown in the middle and bottom plots, respectively.

After the comparisons of the bottom plots of Figs. 10 to 12, it is found that all the computer simulations have the same time history of step error. This implies that each simulation will have the same simulation errors for exploring the error propagation effect. In Fig 10, the simulation results for M4, M5 and M6 are, in general, consistent with the exact solution for the linear elastic system. However, it seems that the simulation result for M4 has more significant high frequency fluctuation when compared to the results for M5 and M6. This is also manifested from the middle plot of this figure. Furthermore, this phenomenon is in good agreement with the error propagation results shown in Figs. 3 and 4, where M4 possesses the largest error amplification factors while M6 has the smallest ones for a given value of Ω_0 . Similar phenomena can be also observed in Figs. 11 and 12. This implies that the cases of instantaneous stiffness softening and hardening will show similar error propagation characteristics as in the case of a linear elastic system. In Fig 12, it is found that numerical instability occurs in the early response of the simulation

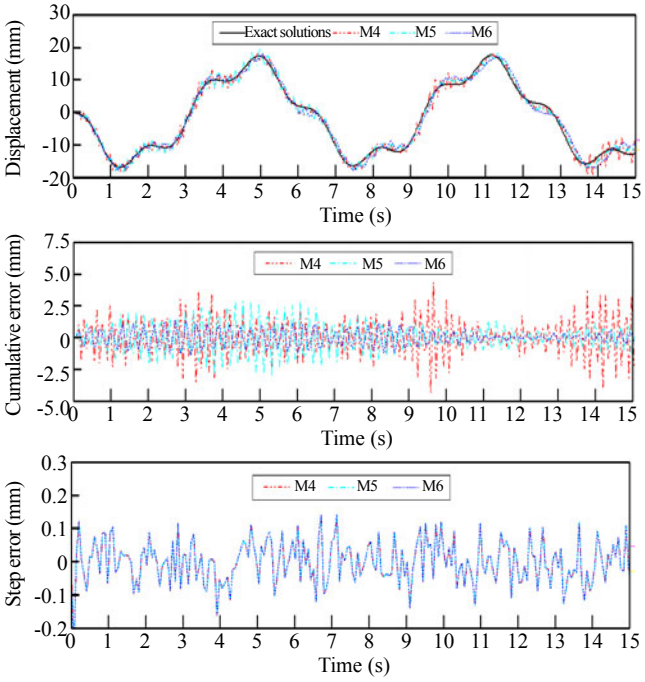

Fig. 10 Computer simulation results for pseudodynamic testing of Sys-1

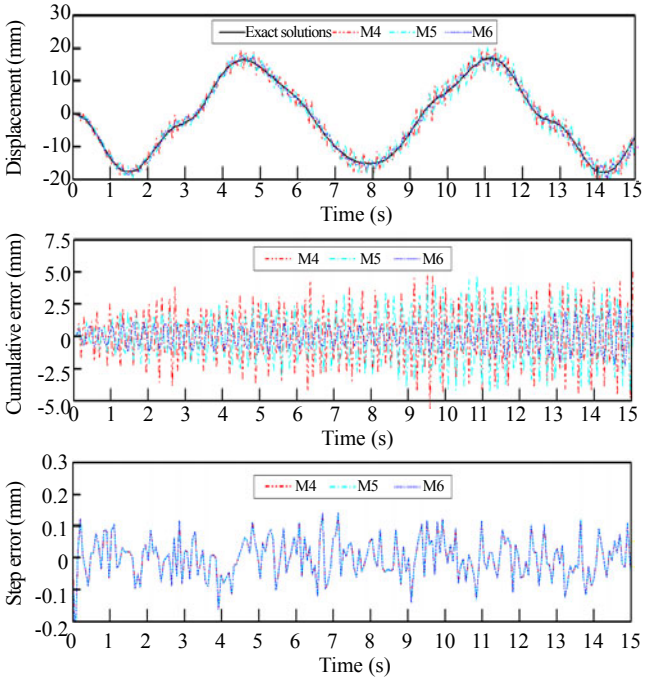

Fig. 11 Computer simulation results for pseudodynamic testing of Sys-2

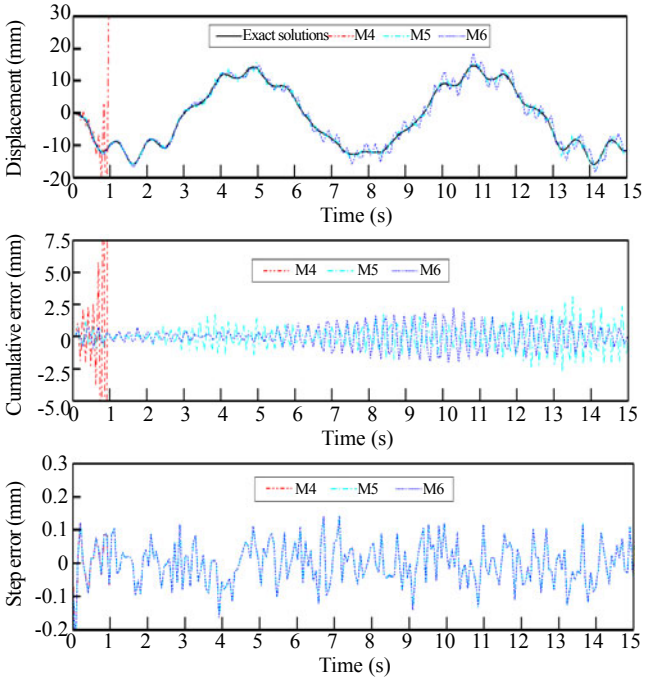

Fig. 12 Computer simulation results for pseudodynamic testing of Sys-3

result for M4 since it is only of conditional stability and the upper stability limit is violated.

10 Pseudodynamic tests

A series of pseudodynamic tests were performed to confirm the feasibility of the proposed family algorithm. Some steel beams with a cross section of H200×200×8×12 and a length of 3.2 m were adopted for the tests. A cantilever beam was designed and fabricated and is simulated as a 3-DOF system. The experimental setup is shown in Fig. 13 where the cantilever beam is loaded by three actuators in parallel to simulate a 3-DOF system. The steel beam is loaded in its minor axis so that the problem of local buckling or instability can be avoided. A small linear elastic range was found for the specimen due to the relatively large dimension of the cross section, very rigid connections and the tightened swivel of each actuator.

It is necessary to obtain the initial stiffness matrix to use the proposed family algorithm before performing an actual pseudodynamic test. As a result, the initial stiffness matrix of the specimen is experimentally obtained as follows

$$\boldsymbol{K}_0 = \begin{bmatrix} 66.2 & -50.0 & 12.8 \\ -50.0 & 71.0 & -31.9 \\ 12.8 & -31.9 & 20.7 \end{bmatrix} \tag{33}$$

where the unit for all elements is in kN/mm. The measured off-diagonal term k_{ij} is not exactly equal to k_{ji} for $i \neq j$. However, an average value is taken so that a symmetric stiffness matrix can be obtained. This symmetric matrix will be used to compute the coefficient matrices. The lumped masses for the first, second and third degree-of-freedom are taken to be 4.0×10^5, 2.0×10^3 and 6.0×10^4 kg. Consequently, the natural frequencies of the system are found to be 5.25, 12.48 and 189.28 rad/s.

The specimen is subjected to the 1995 Kobe earthquake with a peak ground acceleration (PGA) of 0.0015 g for linear tests while for inelastic tests the PGA is scaled to 0.05 g. Figure 14 shows the linear test results and the inelastic test results are shown in Fig. 15. Pseudodynamic results for M1 with a time step of

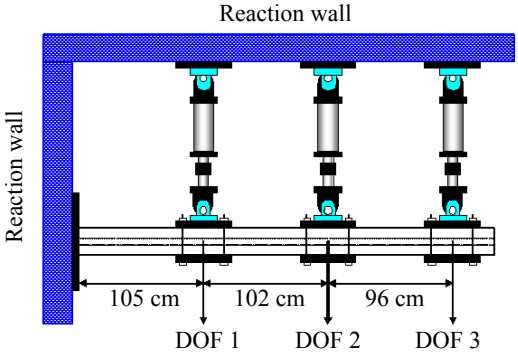

Fig. 13 Pseudodynamic test setup for cantilever beam

Δt = 0.005 s are considered as "correct" solutions for comparison. For this time step, the values of $\Delta t / T_0$ for all three modes are found to be 0.0042, 0.010 and 0.15. This implies that the first two modes are accurately integrated. Although a considerable period distortion is found for the third mode, its contribution is insignificant and thus very reliable solutions can be obtained.

In performing the pseudodynamic tests, M1, M4 and M6 are used to carry out the step-by-step integration. It is found in Figs. 14 and 15 that instability occurs in the

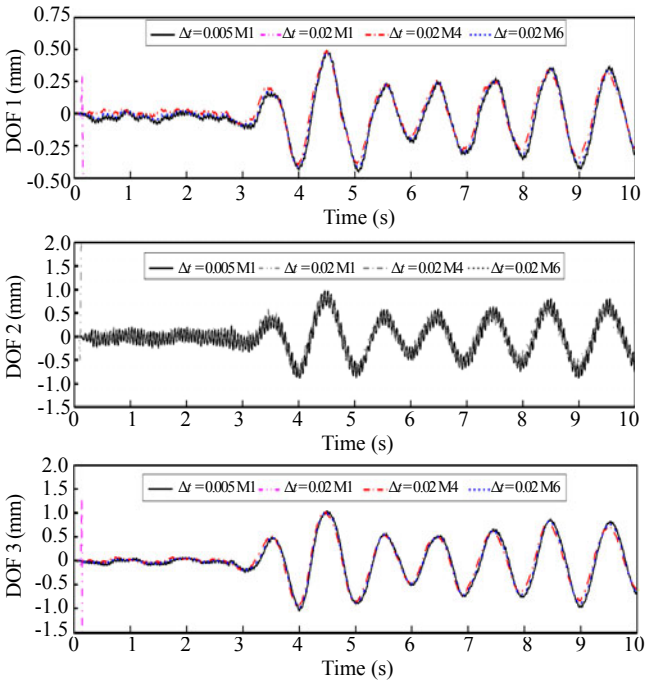

Fig. 14 Pseudodynamic results for system subject to 0.0015 g Kobe earthquake

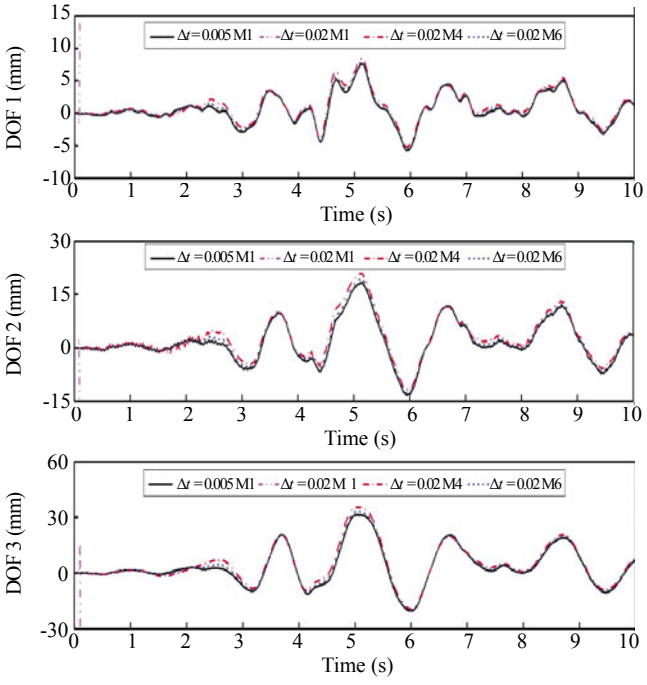

Fig. 15 Pseudodynamic results for system subject to 0.05g Kobe earthquake

very early responses if using M1 with a time step of Δt = 0.02 s while M4 and M6 still provide reliable results. This is because the value of $\Omega_0^{(3)}$ for the third mode is equal to 3.79, which is larger than the upper stability limit 2.0 for M1. Thus, instability occurs. On the other hand, it is indicated that M4 and M6 can be of unconditional stability for an instantaneous stiffness softening system and a linear elastic system since acceptable results can still be achieved for the value of $\Omega_0^{(3)}$ =3.79 for both the linear elastic and inelastic tests.

11 Conclusions

A novel family of explicit pseudodynamic algorithms is presented herein. Since the proposed family algorithm has the same characteristic equation as the Newmark family method for a linear elastic system, it naturally inherits the same numerical properties as those of the Newmark family method at least for linear elastic systems. Due to excellent stability properties, a subfamily of this proposed family algorithm has been shown to be very suitable for use in general pseudodynamic testing, where the total response was dominated by low frequency modes while the high frequency responses are of no interest. In fact, this subfamily offers unconditional stability for any instantaneous stiffness softening systems, any linear elastic systems and instantaneous stiffness hardening systems that may be experienced in practice when performing a pseudodynamic test. This implies that it is not necessary to consider the stability problem to conduct a general pseudodynamic test if this subfamily is used.

In addition to the favorable stability characteristics, the proposed family algorithm can offer similar accuracy when compared to second-order accurate methods for both linear elastic and nonlinear systems. It seems that the proposed approximate guideline of choosing an appropriate time step to satisfy $\Delta t / T_0 < 0.05$ for the modes of interest works well for both linear elastic and nonlinear systems. The subfamily for the β value in the range of $\frac{1}{3} \le \beta \le \frac{1}{2}$ or $\frac{1}{3} \le \beta \le \frac{2}{3}$ and $\gamma = \frac{1}{2}$ also has improved error propagation properties when compared to M4. This is manifested from error propagation analysis and a series of numerical simulations. Finally, the explicitness of each time step enables it to have an explicit implementation for the general pseudodynamic testing. The feasibility of this proposed family algorithm is also pseudodynamically confirmed.

Acknowledgement

The author is grateful to acknowledge that this study is financially supported by the Science Council, Chinese Taipei under Grant No. NSC-95-2221-E-027-099.

References

Belytschko T and Hughes TJR (1983), Computational Methods for Transient Analysis, Elsevier Science Publishers B.V., North-Holland.

Chang SY (1996), "A Series of Energy Conserving Algorithms for Structural Dynamics," *Journal of the Chinese Institute of Engineers*, **19**(2): 219–230.

Chang SY (1997), "Improved Numerical Dissipation for Explicit Methods in Pseudodynamic Tests," *Earthquake Engineering and Structural Dynamics*, **26**: 917–929.

Chang SY (2000), "The γ–function Pseudodynamic Algorithm," *Journal of Earthquake Engineering*, **4**(3): 303–320.

Chang SY (2001), "Application of the Momentum Equations of Motion to Pseudodynamic Testing," *Philosophical Transactions of the Royal Society*, Series A, **359** (1786): 1801–1827.

Chang SY (2002), "Explicit Pseudodynamic Algorithm with Unconditional Stability," *Journal of Engineering Mechanics*, ASCE, **128**(9): 935–947.

Chang SY (2003), "Nonlinear error propagation analysis for explicit pseudodynamic algorithm," *Journal of Engineering Mechanics*, ASCE, **129**(8): 841-850.

Chang SY (2005), "Error propagation in implicit pseudodynamic testing of nonlinear systems," *Journal of Engineering Mechanics*, ASCE, **131**(12): 1257–1269.

Chang SY (2007), "Improved Explicit Method for Structural Dynamics," *Journal of Engineering Mechanics*, ASCE, **133**(7): 748–760.

Chang SY and Mahin SA (1993), "Two New Implicit Algorithms of Pseudodynamic Test Methods," *Journal of the Chinese Institute of Engineers*, **16**(5): 651–664.

Chang SY, Tsai KC and Chen KC (1998), "Improved Time Integration for Pseudodynamic Tests," *Earthquake Engineering and Structural Dynamics*, **27**: 711–730.

Chung J, and Hulbert GM (1993), "A Time Integration Algorithm for Structural Dynamics with Improved Numerical Dissipation: the Generalized-α method," *Journal of Applied Mechanics*, **60**(6): 371–375.

Hilber HM, Hughes TJR, and Taylor RL (1977), "Improved Numerical Dissipation for Time Integration Algorithms in Structural Dynamics," *Earthquake Engineering and Structural Dynamics*, **5**: 283–292.

Houbolt JC (1950), "A Recurrence Matrix Solution for the Dynamic Response of Elastic Aircraft," *Journal of the Aeronautical Sciences*, **17**: 540–550.

Hughes TJR (1987), *The Finite Element Method*, Prentice-Hall, Inc., Englewood Cliffs, N.J., U.S.A.

Nakashima M, Kaminosomo T and Ishida M (1990), "Integration Techniques for Substructure Pseudo-Dynamic Test," *Proceeding of Fourth U.S. National Conference on Earthquake Engineering*, **2**: 515–524.

Newmark NM (1959), "A Method of Computation for Structural Dynamics," *Journal of Engineering Mechanics Division*, ASCE, **85**: 67–94.

Park KC (1975), "An Improved Stiffly Stable Method for Direct Integration of Nonlinear Structural Dynamic Equations," *Journal of Applied Mechanics*, **42**: 464–470.

Peek R and Yi WH (1990a), "Error Analysis for Pseudodynamic Test Method. I: Analysis," *Journal of Engineering Mechanics*, ASCE, **116**: 1618–1637.

Peek R and Yi WH (1990b), "Error Analysis for Pseudodynamic Test Method. II: Application," *Journal of Engineering Mechanics*, ASCE, **116**: 1638–1658.

Shing PB and Mahin SA (1987a), "Cumulative Experimental Errors in Pseudodynamic Tests," *Earthquake Engineering and Structural Dynamics*, **15**: 409–424.

Shing PB and Mahin SA (1987b), "Elimination of Spurious Higher-mode Response in Pseudodynamic Tests," *Earthquake Engineering and Structural Dynamics*, **15**: 425–445.

Shing PB and Mahin SA (1990), "Experimental Error Effects in Pseudodynamic Testing," *Journal of Engineering Mechanics*, ASCE, **116**: 805–821.

Shing PB and Manivannan T (1990), "On the Accuracy of an Implicit Algorithm for Pseudodynamic Tests," *Earthquake Engineering and Structural Dynamics*, **19**: 631–651.

Shing PB, Vannan MT and Carter E (1991), "Implicit Time Integration for Pseudodynamic Tests," *Earthquake Engineering and Structural Dynamics*, **20**: 551-576.

Thewalt CR and Mahin SA (1995), "An Unconditionally Stable Hybrid Pseudodynamic Algorithm," *Earthquake Engineering and Structural Dynamics*, **24**: 723–731.

Wood WL, Bossak M, and Zienkiewicz OC (1981), "An Alpha Modification of Newmark s Method," *International Journal for Numerical Methods in Engineering*, **15**: 1562–1566.